Role of Charged Residues in the Catalytic Mechanism of Hepatitis C Virus NS3 Protease: Electrostatic Precollision Guidance and Transition-State Stabilization

Uwe Koch, Gabriella Biasiol, Mirko Brunetti, Daniela Fattori, Michele Pallaoro, and Christian Steinkühler*

Istituto di Ricerche di Biologia Molecolare (IRBM) "P. Angeletti", Via Pontina Km 30,600, 00040 Pomezia, Italy

Received September 13, 2000

ABSTRACT: Maturational cleavage of the hepatitis C virus polyprotein involves the viral chymotrypsin-like serine protease NS3. The substrate binding site of this enzyme is unusually flat and featureless. We here show that NS3 has a highly asymmetric charge distribution that is characterized by strong positive potentials in the vicinity of its active site and in the S5/S6 region. Using electrostatic potential calculations, we identified determinants of this positive potential, and the role of six different residues was explored by site-directed mutagenesis. Mutation of residues in the vicinity of the active site led to changes in k_{cat} values of a peptide substrate indicating that basic amino acids play a role in the stabilization of the transition state. Charge neutralization in the S5/S6 region increased the K_m values of peptide substrates in a manner that depended on the presence of negatively charged residues in the P5 and P6 positions. K_i values of hexapeptide acids spanning P6−P1 (product inhibitors) were affected by charge neutralization in both the active site region and the S5/S6 region. Pre-steady-state kinetic data showed that the electrostatic surface potential is used by this enzyme to enhance collision rates between peptidic ligands and the active site. Calculations of the interaction energies of protease−substrate or protease−inhibitor complexes showed that electrostatic interaction energies oppose the formation of a tightly bound complex due to an unfavorable change in the desolvation energy. We propose that desolvation costs are minimized by avoiding the formation of individual ion pair interactions through the use of clusters of positively charged residues in the generation of local electrostatic potentials.

The replication of the hepatitis C virus (HCV[1]), an important human pathogen, crucially depends on the proteolytic maturation of a large viral polyprotein precursor. The viral nonstructural protein 3 (NS3) harbors a serine protease domain that plays a key role in this process, being responsible for four out of the five cleavage events that occur in the nonstructural region of the HCV polyprotein. The NS3 protein is a multifunctional polypeptide containing both a serine protease and an RNA helicase (*1*−*6*). The two enzymatic functions of the NS3 protein are presently the focus of intensive research since their inhibition is considered as a possible strategy for the development of antiviral pharmaceuticals (*7*−*9*).

The full proteolytic activity of NS3 is attained only upon binding of the protease to the viral protein NS4A (*10*−*13*). Synthetic peptides spanning the central, hydrophobic region of NS4A (residues 21−34) were shown to elicit full activation of the purified NS3 protein in vitro (*14*−*19*). The X-ray crystal structures of the uncomplexed protease domain and of the binary serine protease-cofactor peptide complex have been determined (*1*−*3*). In addition, an NMR solution structure of the free enzyme has been obtained (*20*). Analysis of these structures led to the proposal that the cofactor activates the enzyme by stabilizing the fold of its N-terminal domain that contains both residues involved in catalysis and in substrate recognition.

The NS3 protease has a rather peculiar substrate specificity, requiring relatively large, at least decamer, peptide substrates spanning from P6 to P4′ (*21*−*23*). This requirement for large substrate molecules is a result of a flat and featureless substrate binding site, the binding energy being derived from a series of weak interactions distributed along this contact surface. Conserved features of NS3 protease substrates involved in this recognition process are as follows: a negatively charged residue in P6, the preference for a cysteine in P1, and a hydrophobic residue in the P4′ position. Besides the acidic residue in P6, some NS3 substrates also contain an additional, negatively charged residue in the P5 position. Deletion of the acidic residues was shown to lead to increased K_m values (*21*). Similar effects were observed upon charge neutralization or inversion in this position (*22*). In addition, K_m values of all NS3 substrates were shown to increase with increasing ionic strength (*23*). These findings suggest that electrostatic interactions involving at least the P6 acid are important driving forces in the substrate recognition process. Molecular modeling and NMR data in addition to recent crystallographic data have shown that the P6 residue is likely to bind to a region of the protease that is characterized by a clustering of positively charged amino acids, and among these, residues K165 and R161 were indicated as possible candidates for a specific interaction (*6*, *24*, *25*).

* To whom correspondence should be addressed. Phone: ++39 06 91093232. Fax: ++39 06 91093225. E-mail: Christian_Steinkuhler@Merck.com.

[1] Abbreviations: Cha, cyclohexylalanine; CHAPS, 3-[(3-cholamidopropyl)dimethylammoniol-1-propanesulfonate; Dap, diaminoproprionic acid; DTT, dithiothreitol; HCV, hepatitis C virus; Hepes, *N*-(2-hydroxyethyl)piperazine-*N*′-2-ethanesulfonic acid; HPLC, high-performance liquid chromatography; NS, nonstructural; PCR, polymerase chain reaction; TFA, trifluoracetic acid.

10.1021/bi002160t CCC: $20.00
Published on Web 12/23/2000

The NS3 protease is subject to a remarkable inhibition by its N-terminal cleavage products (*26*, *27*). The interaction of hexamer peptide acids spanning from P6 to P1, derived from the cleavage products of substrate peptides harboring sequences of the natural cleavage sites, have been extensively studied using kinetic methods (*26*), site-directed mutagensis (*26*), and NMR (*24*, *25*). In addition, structure−activity relationships were established using both combinatorial techniques (*28*) and systematic modifications (*27*, *28*). According to these studies, product inhibitors bind to the active site of the enzyme in an extended conformation, contacting strand E2 of the protease. The strength of the interaction appears to crucially rely on two electrostatic interactions: one similar to that encountered in the substrate and involving the P6 acidic residue and the other one mediated by the P1 α carboxylate (*28*). NMR data, molecular modeling, pH titration experiments, and site-directed mutagenesis (*24*−*26*) have shown that this carboxylic acid most likely engages in hydrogen bond interactions with the amide groups forming the so-called oxyanion hole, the protonated ϵ-N of the catalytic His57 and the side chain of Lys136 (*26*). As observed with substrate peptides, also the affinities for product inhibitors decrease with increasing ionic strength in a fashion that somewhat correlates with the charge density on the inhibitor molecule (*28*). The available data point to a pivotal contribution of electrostatic interactions in enzyme−inhibitor complex formation.

In the present work, we have attempted to gain a deeper insight into the role of electrostatics in active site ligand binding and catalysis by the NS3 protease and analyzed the role of six different, positively charged residues in the interaction of the enzyme with substrates or product inhibitors using site-directed mutagenesis. We show that electrostatic interactions play a role in the catalytic mechanism and are used by this enzyme to increase the rate of productive collisions with the active site region. In the absence of well-defined substrate binding pockets, specificity and affinity are conferred to the recognition process through the selective attraction of ligands whose charge distribution is complementary to that of the active site of the enzyme.

MATERIALS AND METHODS

Enzyme Preparations and Steady-State Kinetic Measurements. The NS3 protease domain from the HCV J strain encompassing amino acids 1027−1206 of the viral polyprotein was purified from *Escherichia coli* as previously described (*29*). Point mutations were generated by PCR using mutagenic primers. The following rationale was used in the mutagenesis strategy: Residues K136 and R109 are located in the active site region and were mutated into methionine and glutamine, respectively, thereby conserving the hydrophobic side chains in these positions. R155 is located in a position where a serine residue is usually found in other proteases of the chymotrypsin family (Ser214 in chymotrypsin). It was therefore mutagenized into serine. R123 is highly but not absolutely conserved throughout all HCV isolates, and a threonine residue is found in this position in some strains. This amino acid was therefore chosen to substitute the arginine present in the position 123 of the HCV J strain NS3 protease. Residues R161 and K165 are highly solvent exposed, and R161 is located at the tip of a short hairpin loop. Serine appeared to be the most appropriate substitution in these positions. cDNAs were fully sequenced on both strands in order to ensure that no additional mutations were introduced by errors of the Taq polymerase. In addition, the purified enzymes were characterized by N-terminal sequence analysis using Edman degradation on an Applied Biosystems model 470A gas-phase sequencer and by electrospray mass spectrometry done on a Perkin-Elmer API 100 instrument. All proteins showed N-terminal sequence heterogeneity with up to 80% of the molecules starting with Met1. All synthetic peptides were bought from AnaSpec. As protease cofactor, we used a peptide spanning the central hydrophobic core (residues 21−34) of the NS4A protein containing a solubilizing lys-tag at its N-terminus [Pep4AK (KKKGSVVIVGRIILSGR(NH_2)] (*18*). Activity assays were done in 50 mM Hepes (pH 7.5), 1% CHAPS, 1 mM DTT, and 15% glycerol containing 80 μM Pep4AK using a synthetic substrate peptide corresponding to the NS5A/NS5B junction of the HCV polyprotein (Pep5AB, EAGDDIVPC-SMSYTWTGA-OH). An enzyme concentration of 2−10 nM was used in these experiments. Reactions were performed at 23 °C, stopped by the addition of TFA, and analyzed by HPLC (*22*). K_m values were determined by nonlinear least-squares fit of substrate titration data to the Michaelis−Menten equation, using a Kaleidagraph software. K_i values were calculated from IC_{50} values obtained from inhibitor titration experiments performed at [S] = K_m as previously described (*30*).

The change of the free enthalpy of binding $\Delta\Delta G_{binding}$ was calculated from K_m or K_i values according to

$$\Delta\Delta G_{binding} = RT \ln(K_{mutant}/K_{wild-type}) \quad (1)$$

Pre-Steady-State Measurements. Association rate constants of the fluorescent active site probe **P** (Ac-D-E-Dap(*N*-β-dansyl)-E-Cha-C-OH) (*31*) were measured on an SX-MV18 Applied Photophysics stopped-flow instrument equipped with a fluorescence detector and interfaced with a Risc computer. The samples and the flow cell were thermostated at 23 °C. To 70−200 nM protease in 50 mM Hepes (pH 7.5), 1 mM DTT, 15% glycerol, and 1% CHAPS containing 80 μM NS4A cofactor peptide (final concentrations) increasing concentrations of **P** were added. Under these conditions, we measured a dead time of 1.8 ms with a standard reference reaction (reduction of 2,6-dichlorindophenol by ascorbic acid, ref *32*). Protein fluorescence was excited at 280 nm, and a 400-nm cutoff filter was used to suppress both the excitation wavelength and the tryptophan emission band. Observed rate constants were obtained by fitting experimental data with a single-exponential equation by least squares nonlinear regression analysis. k_{obs} values derived from this fitting procedure were determined at different concentrations of **P** and used to calculate association rate constants according to

$$k_{obs} = k_{off} + k_{on}[\mathbf{P}] \quad (2)$$

The dissociation rate constant k_{off} was estimated from the *y*-axis intercept of k_{obs} versus [**P**] plots.

Molecular Modeling. The structural data for the complex of the hexapeptide product inhibitor and the NS3 protease with its cofactor NS4A were taken from the solution structure of the corresponding complex in the absence of NS4A (*24*). In the solution structure, the S-site of the NS3 protease ligand

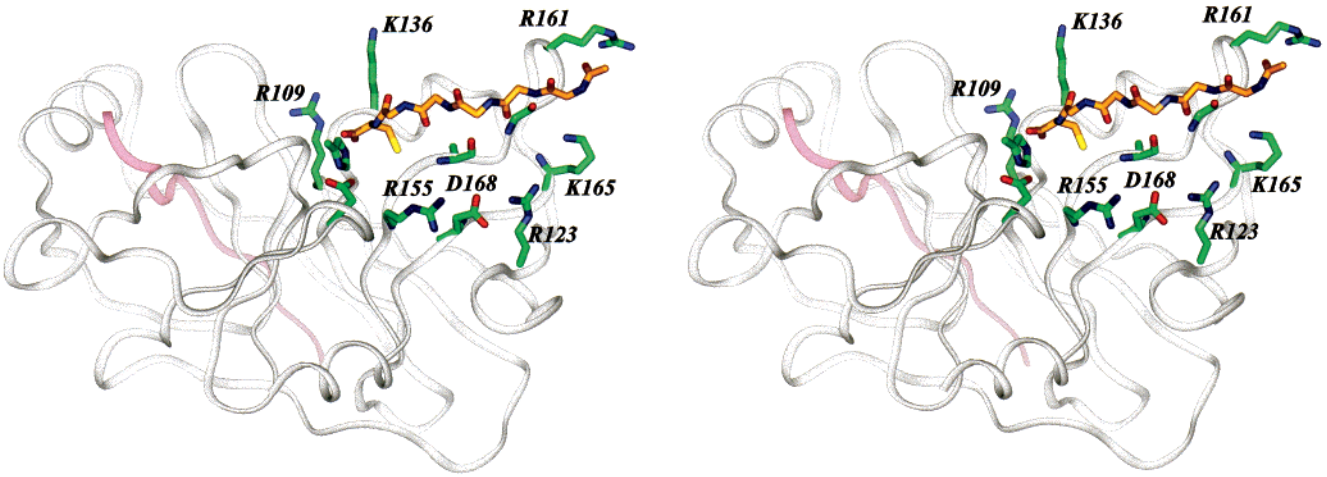

FIGURE 1: Ribbon representation of the backbone of the crystal structure NS3 protease/NS4A complex with the backbone of a hexapeptide product inhibitor. The amino acids discussed are also shown.

binding region without the cofactor NS4A and the crystal structure of the NS3/NS4A complex (*3*) are very similar so that the structural data for the product inhibitor are transferable to the complex. Since NMR data for a substrate molecule bound to the NS3 protease were not available, the solution structure of the product inhibitor complex was used to define the interactions and conformation of the P site of the substrate Pep5AB. To study the transition state the P1 amide was modeled as a tetrahedral transition state intermediate with a covalent bond formed between the catalytic triad S139 γ-O and the amide carbon. The P′ site of the substrate was attached in an extended conformation and subsequently optimized by a combination of molecular dynamics and energy minimization. All calculations were carried out with the program BatchMin and the molecular modeling package InsightII/Discover (Biosym Technologies Inc., San Diego, CA). Hydrogen atoms were included, and the potential energy of the complex was expressed by the force field MMFF (*33*) with the generalized Born/surface area implicit solvation model (*34*) as implemented in the MacroModel V5.0 distribution of the simulation program Batchmin. No nonbonded or Coulombic cutoffs were used. For the dielectric constant of the solute the default value (1.0) for which this force field has been validated (*35*) was used.

Electrostatic potentials and electrostatic interaction energies were calculated with the DelPhi software package (*36*), which solves the nonlinear Poisson Boltzmann equation by the finite difference method. The calculation employed a grid of 153 × 153 × 153 with a grid resolution of 0.4 Å. We decided to set the solvent dielectric constant to 80 and the solute dielectric constant to 4.0 since these values are in widespread use for the treatment of proteins using these methods, thus allowing a direct comparison with results published elsewhere. No water molecules were explicitly included. Charges were assigned to amino acids charged at a pH of 7.5. A single electronic charge was assigned to the guanidine carbon atom of arginine and the side chain nitrogen atom of lysine. One-half of an electronic charge was assigned to the carboxylate oxygen atoms of aspartate and glutamate and, if protonated, to the imidazol nitrogen atoms of His. Changes in the protonation state of mutagenized amino acids due to changes of electrostatic interactions were estimated by calculating the pK_a shifts for these residues in the wild type and mutants and adding those to the reference state (*37*, *38*). H57 was considered uncharged in the free enzyme where a pK_a of 6.8 has been measured (*39*) and in the complex with Pep5AB. For the calculations of the transition state and the interactions with the hexapeptide product inhibitors, H57 was treated as protonated. The transition-state oxyanion was considered to be negatively charged. It was not tried to take into account the effect of pK_a shifts for the transition-state oxyanion since the pK_a of the reference state is not exactly known. For each calculation, the crystal structure of the free NS3/NS4A complex (*3*, *40*) was used. With the exception of K136, no attempts were made to take conformational changes into account.

To calculate changes in the electrostatic energy due to single mutations, the contribution of that residue was calculated according to

$$\Delta G_{el} = \frac{1}{2}\sum_i q_i \Delta\phi_i^{rxn} + \sum_i q_i \, \Delta\phi_i^{int} \qquad (3)$$

The sum is over all charges in the free enzyme and the complex. The first term is the residue's contribution to the solvation energy, and the second term is to the charge−charge interaction. The second term was further divided into an intermolecular contribution, the change in interaction energy between the protein and the ligand upon mutation, and the change of the intramolecular interactions (*41*, *42*). The change in the free binding energy due to a mutation ($\Delta\Delta G_{el}$) was calculated in each case as the difference in the electrostatic binding energies of the wild type and the mutagenized enzyme. The atomic radii were taken from the CFF91 parameter set.

RESULTS

Overall Structure of Complex between NS3 Protease and a Product Inhibitor. In Figure 1, a ribbon representation of the NS3 protease/NS4A complex is shown together with the backbone atoms of a hexapeptidic product inhibitor. The mode of binding of product inhibitors and substrates on the

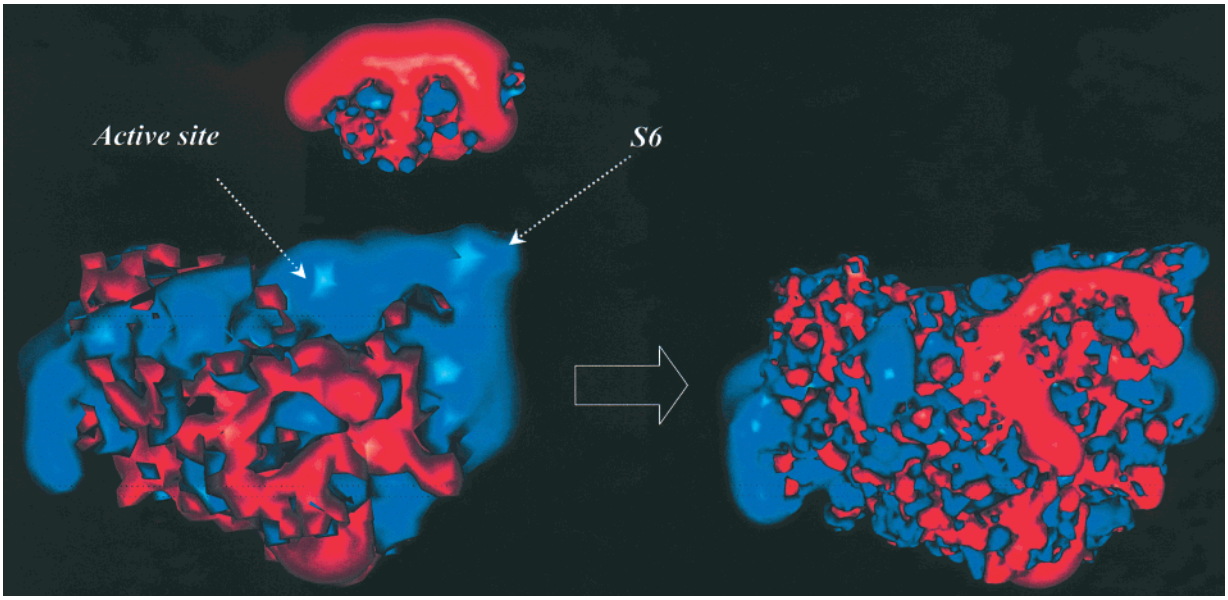

FIGURE 2: Electrostatic potential for the NS3 protease/NS4A complex and the product inhibitor Ac-Asp-Glu-Dif-Glu-Cha-Cys-OH separated (left) and for the NS3/NS4A/product inhibitor complex (right). The average potential is contoured at 2.5 (blue) and −2.5 kJ mol^{-1} (red).

S-site of the substrate binding site is assumed to be very similar. Figure 1 illustrates how shallow and solvent exposed the substrate binding region is.

Electrostatic Properties of NS3 Protease. The presence of a number of highly conserved acidic amino acids in the substrates and the most potent product inhibitors as well as the importance of product inhibition itself (*26*, *27*) suggest that the electrostatic properties of the NS3 protease could be important to understand the binding modes of substrates or of small peptidic inhibitors. We have therefore analyzed the electrostatic potential of the NS3 protease using the program DelPhi (*36*). The analysis reveals a charge distribution rather unusual for serine proteases. The electrostatic potential of the enzyme is in fact characterized by strong positive potentials in the vicinity of its active site and in the S5/S6 region (Figure 2). The electrostatic potential of the hexapeptide product inhibitor Ac-Asp-Glu-Dif-Ile-Cha-Cys-OH is complementary to the potential of the protease in the substrate binding region (Figure 2). Thus, the lack of well-defined binding pockets seems to be compensated by a high degree of electrostatic complementarity. The nonuniform electrostatic potential of the protease is caused by two clusters of basic amino acids: close to the active site there are K136, R155, and R109; close to S5/S6, six basic amino acids contribute to the positive electrostatic potential in this area (R161, K165, R130, R123, R119, and R117). In the sequences of the natural substrates, this charge distribution is reflected by the presence of a conserved acidic amino acid (Glu or Asp) in P6. The most potent hexapeptide product inhibitors and substrates contain in addition an acidic amino acid in P5. We believe the P5/P6 acidic amino acids to act as an anchor for both the substrate and the product inhibitors.

We next decided to explore the role of the positively charged residues in the substrate binding site of the NS3 protease experimentally, using site-directed mutagenesis. Three different ligands were used to probe the effect of the mutations: The influence of the charge interactions involving the P5/P6 acids was investigated using the substrate peptide Pep5AB, having the sequence EAG**DD**IVPC−SMSYTWTGA-OH (the acidic P6/P5 couple is in bold, the scissible bond is indicted by a dash between C and S), based on the NS5AB cleavage site of the HCV polyprotein. The influence of electrostatic interactions in the recognition of product inhibitors was explored using the hexapeptide acid Ac-DEDifEChaC-OH and the fluorescently labeled hexapeptide acid Ac-DEDap(*N*-β-dansyl)EChaC-OH, termed compound **P** (*31*). Binding of **P** to the NS3 protease can be directly monitored via fluorescence resonance energy transfer between the dansyl residue of the peptide and protein tryptophan residues (*31*).

Influence of Mutations of Charged Residues of NS3 on Interaction with Pep5AB. The influence of six single and two double mutations, affecting charged residues of NS3, was investigated using Pep5AB (Figure 3A,B). None of the six single or two double mutations significantly affected the affinity of the enzyme for the NS4A cofactor peptide or its fluorescence emission spectra (not shown). Furthermore, we verified that the K136M mutation did not affect the thermostability of the protein (not shown). These data indicate that no macroscopic alteration of the protein structure took place as a consequence of mutagenesis. The mutations gave effects on both k_{cat} and K_m values that will be analyzed in the following.

Influence of Mutations on k_{cat} Values. Mutagenesis of residues 123, 161, and 165, which are distant from the active site, did not significantly affect k_{cat} values (Figure 3A). Mutagenesis of residues R155 or R109 lead to a slight decrease in k_{cat} values (21% and 40%, respectively). The K136M mutation, either alone or in combination with the R109Q mutation, resulted in a pronounced, 4.2- and 8.4-fold decrease in the k_{cat} value, respectively. To better understand this effect, the electrostatic interaction energies between R109, K136, and R155 and the transition-state oxyanion were calculated. For this purpose, Pep5AB was modeled into the ligand binding site with a covalent bond between the γ-O atom of S139 and the amide C-atom of the P1-Cys so that a tetrahedral transition state is formed (Figure 4). The electrostatic interactions were calculated between the

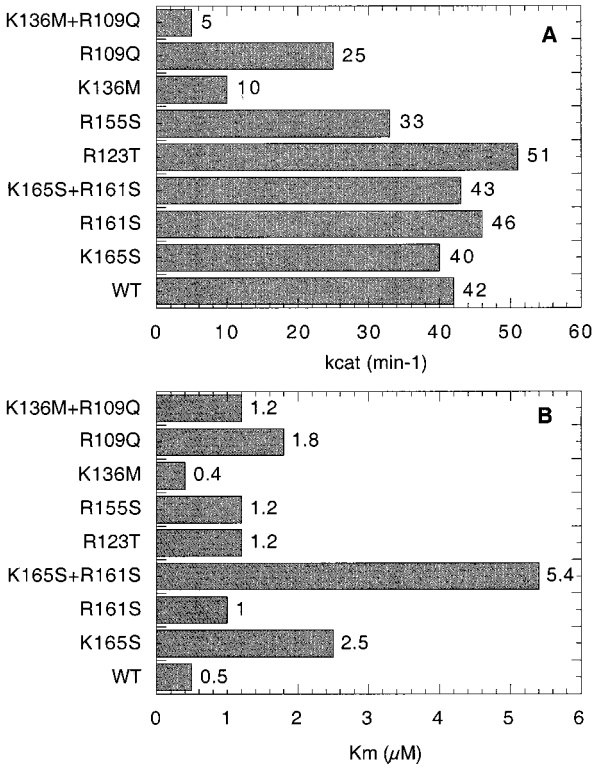

FIGURE 3: Effect of mutations of positively charged residues in the NS3 protease on the interaction with a substrate peptide; 2−10 nM wt or mutant NS3 protease in 50 mM Hepes (pH 7.5), 1% CHAPS, 1 mM DTT, 15% glycerol, and 80 μM Pep4AK were titrated with a synthetic substrate peptide corresponding to the NS5A/NS5B junction of the HCV polyprotein (Pep5AB, EAGDDIVPCSMSYTWTGA-OH). Substrate cleavage was assessed by HPLC, and data were fitted to the Michaelis Menten equation to obtain values for k_{cat} (A) and K_m (B).

oxyanion oxygen and the side chains R109, K136, and R155 (Table 1). Because the mobility of K136 was found to be high in the crystal and solution structures (*3*, *24*, *40*), two different conformations were considered. In one case, all dihedral angles of the K136 side chain were set to 180°corresponding to the most populated conformation in the solution structure ($K136_{(NMR)}$ in Table 1 and Figure 4). In this case, the distance between the charged group of K136 and the oxyanion is relatively large, resulting in an interaction energy similar to that between R109 and the oxyanion. The second conformation corresponds to the orientation found to be favored by modeling due to negatively charged residues in the oxyanion hole. This conformation corresponds to that observed in the crystal structures of the complexes with α-ketoacids ($K136_{(model)}$ in Table 1 and Figure 4). This conformation appears to be stabilized by the attraction between the opposite charges of the oxyanion and K136. Further stabilization is provided by the formation of hydrogen bonds between the γ-NH_3^+ of K136 and the carbonyl oxygen atoms of the P1′ and P2 amide groups (Figure 4). In this conformation, K136 makes an electrostatic contribution to the stabilization of the transition-state oxyanion larger than that of R109 and R155 (Table 1). In addition, K136 also destabilizes the positively charged H57 decreasing its pK_a by 1.5 pH units. This pK_a is further decreased by the presence of R155 (−0.7 pH unit) and R109 (−0.3 pH unit) leading to an overall reduction by 2.5 units. It is noteworthy that the pK_a of the catalytic His of chymotrypsin, which lacks

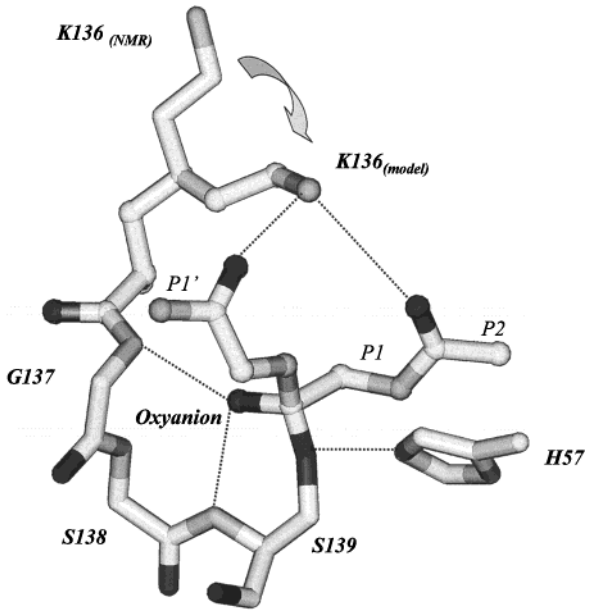

FIGURE 4: Structure of the transition state of substrate cleavage. The transition-state oxygen atom is bound in the oxyanion cavity with hydrogen bonds indicated by dashed lines. K136 is shown in two conformations: one (sticks) corresponding to the solution structure and the other (balls and sticks) corresponding to a conformation favored by the presence of negative charges in the oxyanion hole.

Table 1: Charge−Charge Interaction Energies between Surface Charges at Positions 109, 136, and 155 and the Transition-State Oxyanion (TS) and H57 Calculated with DelPhi at an Ionic Strength of 0.025 mol L^{-1} for Two Different Conformations of K136

	R109 (kJ mol^{-1})	$K136_{(NMR)}$ (kJ mol^{-1})	$K136_{(model)}$ (kJ mol^{-1})	R155 (kJ mol^{-1})
TS	−5.7	−5.4	−25.2	−2.0
His57	1.8	2.4	8.8	4.1

basic amino acids in the vicinity of the active site, has been determined to be between 10.5 and 12 in the presence of transition-state analogues (*43*). A reduction of this value by 2.5 units for NS3 protease due to R109, R155, and K136 gives a value >8 close to where a change in the protonation state at pH 7.5 would be expected. This shift in the pK_a of H57 could explain why the K136M mutation increases the energy barrier to the transition state by only 3.6 kJ mol^{-1}, a value that is smaller than the calculated electrostatic interaction energy between the oxyanion and K136. A reduction in the pK_a of H57 has also been noted in the solution structure of the complex of the NS3 protease with a ketoacid inhibitor. In this case, the pK_a of H57 is reduced from 6.8 in the free enzyme to 5.7 (*39*). However, this result has to be interpreted with the caveat that the ketoacid hemiketal in this structure adopts a configuration that differs from the canonical orientation of the oxyanion expected to occur in the transition state of amide bond scission.

Influence of Mutations on K_m Values. Figure 3B shows the effect of the mutations on the K_m value of substrate Pep5AB. K_m values of amide substrates of the NS3 protease have been shown to reflect the true equilibrium dissociation constants of the enzyme−substrate complex (*22*). Most mutations had rather modest effects on the affinity of the enzyme for Pep5AB. The mutation K165S and the double mutant K165S + R161S resulted in the largest increases (5-

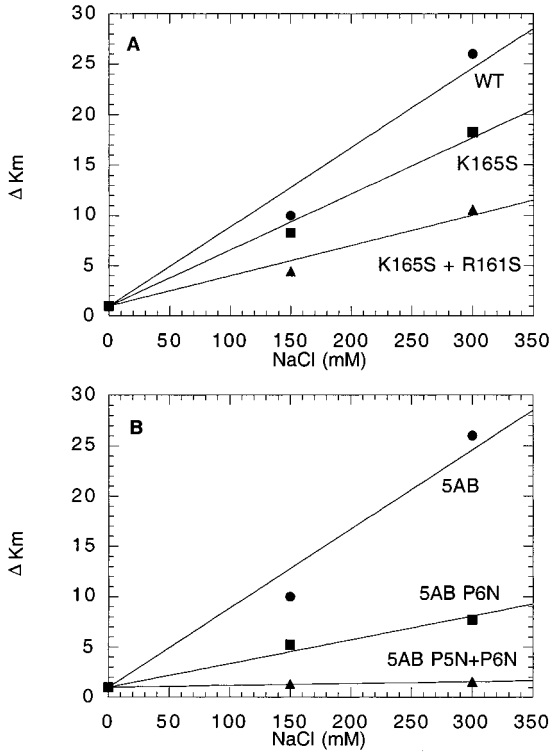

FIGURE 5: Ionic strength dependence of K_m values. (A) Cleavage of the peptide substrate Pep5AB (EAGDDIVPCSMSYTWTGA-OH) by 2−10 nM wt or mutant NS3 protease was assessed in 50 mM Hepes (pH 7.5), 1% CHAPS, 1 mM DTT, 15% glycerol, and 80 μM Pep4AK and upon addition of 150 or 300 mM NaCl. Cleavage kinetics were analyzed as described in the legend of Figure 3. No significant effect of NaCl was noticed on k_{cat} values, whereas K_m values increased with increasing salt concentration. The K_m values obtained in the absence of salt (compare Figure 3B) were normalized, and the salt-dependent K_m increase (ΔK_m) is shown. (B) Cleavage of the peptide substrate Pep5AB EAGDDIVPCSMSYTWTGA-OH (5AB) and of the mutant substrates EAGNDIVPCSMSYTWTGA-OH (5AB P6N) and EAGNNIVPCSMSYTWTGA-OH (5AB P5N + P6N) by the wild-type NS3 protease was assessed as a function of added NaCl. The K_m values obtained in the absence of salt (Table 2) were normalized, and the relative salt dependence (ΔK_m) is shown.

and 10-fold, respectively) of K_m values. Concomitantly, the two mutants showed a diminished sensitivity to increased NaCl concentration if compared to the wild-type enzyme (Figure 5A). These data are indicative of residues K165 and R161 being involved in electrostatic interactions with the substrate. Molecular modeling (Figure 1) as well as structural data (*6*, *24*, *25*) have suggested that K165 may be involved in an interaction with the acidic P6 residue, conserved in most NS3 protease substrates. The role of these electrostatic interactions was further explored by neutralizing the charged P5 and P6 residues in Pep5AB, through substitution of the wild-type aspartic acid residues by asparigine. Both the single and the double modifications were investigated. The introduction of asparagine residues in the P5 and/or P6 positions had no measurable effect on k_{cat} values but resulted in increased K_m values (Table 2). Both acidic amino acids in P5 and P6 contribute equally to the free binding enthalpy. To confirm that the introduction of asparagine residues in the P5 and P6 positions of the substrate was indeed affecting electrostatic interactions with the enzyme, we determined the dependence of the P6N and P5N + P6N-modified substrates on increasing concentrations of NaCl, using the

Table 2: Role of Negatively Charged Residues in the P5 and P6 Positions of an NS5AB Peptide Substrate[a]

substrate	k_{cat} (min^{-1})	K_m (μM)	$\Delta\Delta G_{binding}$ (kJ mol^{-1})
EAGDDIVPC−SMSYTWTGA	42	0.5	
EAGD**N**IVPC−SMSYTWTGA	48	4.1	5.2
EAG**N**DIVPC−SMSYTWTGA	42	3.8	5.0
EAG**NN**IVPC−SMSYTWTGA	40	25.2	9.7

[a] 2 nM NS3 protease in 50 mM Hepes (pH 7.5), 1% CHAPS, 1 mM DTT, and 15% glycerol containing 80 μM Pep4AK were titrated with increasing amounts of substrate peptides. Reactions were stopped at <10% substrate conversion, and samples were analyzed by HPLC. k_{cat} and K_m values were obtained from a fit of the cleavage data to the Michaelis−Menten equation. $\Delta\Delta G_{binding}$ was calculated from K_m values according to eq 1.

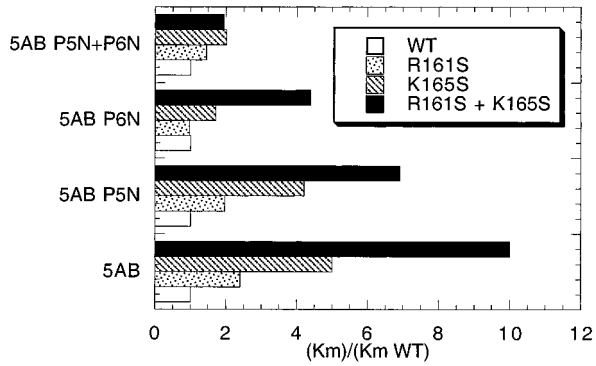

FIGURE 6: Influence of the R161S and K165S mutations on the interaction with substrates modified in the P5 and P6 positions. Assays were performed in 50 mM Hepes (pH 7.5), 1% CHAPS, 1 mM DTT, 15% glycerol, and 80 μM Pep4AK using either wild-type Pep5AB (5AB) or the modified 5AB P5N, 5AB P6N, or 5AB P5N + P6N peptide substrates (compare Table 2 and legend of Figure 5). Each substrate was reacted with the wild type (WT) or the R161S, K165S, or R161S + K165S mutant NS3 proteases, and the kinetic parameters of the reaction were determined as described in the Methods section. K_m values were normalized with respect to the K_m values obtained with the wild-type enzyme that are listed in Table 2.

wild-type enzyme (Figure 5B). As observed upon charge neutralization in the positions 161 and 165 of the enzyme, also charge neutralization in positions P5 and P6 of the substrate resulted in a significantly diminished NaCl sensitivity of the respective K_m values. In fact, the affinity for the substrate with charge neutralization in both P5 and P6 was not affected at all up to an NaCl concentration of 300 mM. We subsequently compared the effects of the mutations R161S, K165S, and R161S + K165S on the wild-type Pep5AB substrate and on the modified substrates with neutralized P5 and P6 charges (Figure 6). Neutralization of the P5 aspartic acid in the P5N substrate only slightly altered the effects of the R161S and K165S mutations in the enzyme. In contrast, the introduction of an asparagine residue in the P6 position of the substrate significantly diminished the effects of the mutations in the enzyme, pointing to an important role of the P6 acidic residue in mediating the electrostatic interactions involving residues R161 and K165. The simultaneous neutralization of both the P6 and the P5 charges abolished any significant effect of the R161S, K165S, and R161S + K165S mutations.

Having demonstrated that significant electrostatic interactions occur between R161 + K165 in the NS3 protease on one hand and the P5 and P6 residues in the substrate on the

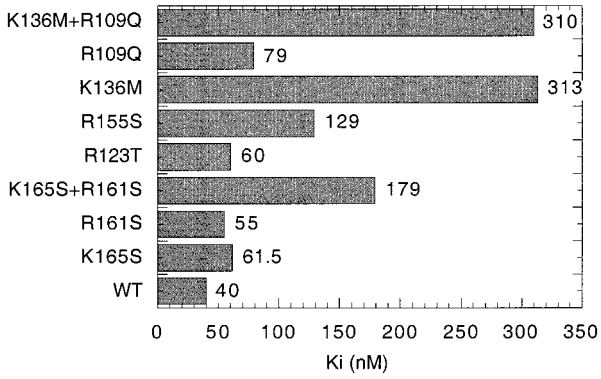

FIGURE 7: Effect of mutations of positively charged residues in the NS3 protease on the interaction with an optimized product inhibitor. To 2−10 nM wt or mutant NS3 proteases incubated in 50 mM Hepes (pH 7.5), 1% CHAPS, 1 mM DTT, 15% glycerol, and 80 μM Pep4AK increasing amounts of the peptide inhibitor Ac-DEDifEChaC-OH were added. K_i values were determined as described in the Methods section.

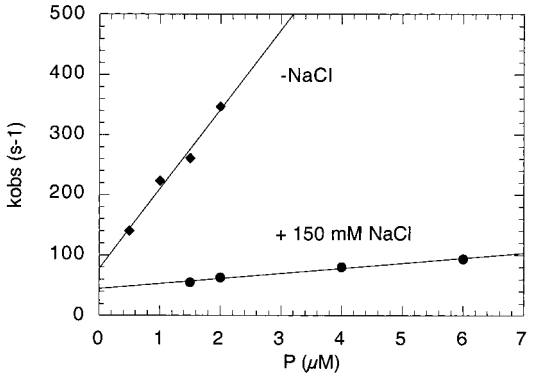

FIGURE 8: Pre-steady-state kinetic analysis of the interaction of the fluorescent inhibitor **P** with the NS3 protease. The interaction of wild-type NS3 protease with the fluorescent ligand **P** was studied in 50 mM Hepes (pH 7.5), 1% CHAPS, 1 mM DTT, 15% glycerol, and 80 μM Pep4AK in the absence or presence of 150 mM NaCl, using a stopped-flow instrument. Association curves were fitted with a single-exponential equation, thereby deriving values for the observed pseudo-first-order association rate constant k_{obs}. k_{obs} values were plotted as a function of the concentration of **P** to obtain values for k_{on} and k_{off} according to eq 2 (Methods section).

other, we wanted to quantify their relative contribution to the overall interaction energy. $\Delta\Delta G$ values were calculated from the K_m values of the wild-type and modified substrates and listed in Tab. 2. The data show that the electrostatic interactions involving the P5/P6 acidic couple contribute to 27% of the total interaction energy (35.9 kJ mol^{-1}) at the investigated ionic strength.

Effect of Charge Mutants on Product Inhibitor Binding. To explore the role of charge−charge interactions in enzyme−inhibitor complex formation with hexapeptide carboxylic acids (product inhibitors), we first used the hexapeptide Ac-DEDifEChaC-OH. The affinity of this compound for our panel of charge mutants of the NS3 protease was determined under steady-state conditions (Figure 7). The affinity pattern turned out to differ substantially from that observed with Pep5AB (Figure 3A). In fact, even though the double mutation R161S + K165S impaired binding of both the product inhibitor and Pep5AB to the enzyme, the major drop in affinity for the inhibitor was observed upon mutagenesis of K136 into methionine, either alone or in the context of the R109Q mutation. K136 was previously proposed to interact with the α carboxylic acid of product inhibitors (*16*). Our data imply that this interaction is more important than the interaction with R161/K165.

We next decided to investigate the interaction of the NS3 protease with a product inhibitor under pre-steady-state conditions. To this purpose, we used a hexapeptide inhibitor, **P**, carrying a fluorescent dansyl label in its P4 position. The fluorescence energy transfer phenomenon between tryptophan residues of the NS3 protease and the dansyl group of bound **P** can be used to determine association rate constants of NS3−**P** complex formation using a stopped-flow instrument (*31*). Plots of k_{obs} versus the concentration of **P** were linear and allowed the calculation of the second-order association rate constants as well as the first-order dissociation rate constants as specified in the methods section. Figure 8 shows an experiment obtained with the wild-type enzyme either in the absence or in the presence of 150 mM NaCl. Table 3 summarizes the results obtained with the wild-type enzyme and the R161S + K165S and K136M mutant enzymes. The second-order association rate constant for the wild-type enzyme (1.5×10^8 M^{-1} s^{-1}) is very fast and its

Table 3: Equilibrium and Pre-Steady-State Parameters of Binding Reaction of Fluorescent Ligand **P** with the NS3 Protease[a]

protein/condition	K_i (μM)	k_{on} (M^{-1} s^{-1})	k_{off} (s^{-1})
WT	0.4	1.5×10^8	70
WT + NaCl	20	1.0×10^6	42
R161S + K165S	3.0	3.0×10^7	82
K136M	30	5.0×10^6	88

[a] K_i values were determined from inhibitor titration experiments performed under equilibrium conditions as described in the Methods section. On and off rates were determined on a stopped-flow instrument.

magnitude suggestive of a diffusion-limited process. In the presence of 150 mM NaCl, the affinity of the enzyme for **P** is decreased 50-fold under equilibrium conditions. Pre-steady-state analysis indicates that this decreased affinity results from a decreased association rate constant (Figure 7 and Table 3), highlighting the importance of electrostatic interactions in driving collision processes between the active site of the NS3 protease and its complementary charged ligands. The drop in affinity for **P** produced by the R161S + K165S and K136M mutations is also attributable to an impairment of the association process.

Molecular Modeling. The interaction energies between the charged residues in the vicinity of the P5 and P6 binding sites were calculated from the experimental K_m values for Pep5AB obtained on the mutant enzymes and compared to the values calculated with DelPhi (Table 4). In accord with experimental data, the charge−charge interaction between K165 and the P5/P6 couple is strongest followed by R155, R123, and R161. In each case however the charge−charge interaction energy is not large enough to compensate the unfavorable change of the solvation energy upon formation of the tight complex. Interestingly some of the charge−charge interactions between oppositely charged amino acids within the ligand binding domain of the NS3 protease, $\Delta\Delta G_{el,intra}$, are enhanced in the low dielectric environment of the complex (Table 4). This is the case for R123, K155, and D168, which are part of a chain of alternatingly charged amino acids (H57, D81, R155, D168, and R123) (Figure 1). A similar effect has been observed for protein−protein interactions (*44*, *45*).

Table 4: Interaction Energies between Surface Charges at Positions 123, 155, 161, 165, and 168 and the P5/P6 Acidic Couple from the Experimentally Determined K_m Values of the Point Mutants and Calculated with DelPhi

	R123 (kJ mol^{-1})	R155 (kJ mol^{-1})	R161 (kJ mol^{-1})	K165 (kJ mol^{-1})	D168 (kJ mol^{-1})
$\Delta\Delta G_{binding}$	−2.1	−2.1	−1.7	−4.0	nd
$\Delta\Delta G$ el,intra[a]	−0.7	−5.1	0.4	0.5	−7.2
$\Delta\Delta G$ el,sum[b]	−6.8	−7.5	−2.2	−9.7	−3.7
$\Delta\Delta G$ solv[c]	118.6	32.1	160.6	192.7	−91.4

[a] Change of intramolecular charge−charge interaction energy upon ligand binding relative to WT-enzyme. [b] Change of intra- and intermolecular charge−charge energy. [c] Change of solvation energy upon ligand binding.

Table 5: Interaction Energies between Surface Charges at Positions 109, 136, and 155 and the P1-Carboxylate from Experimentally Determined K_i Values and Calculated with DelPhi

	R109 (kJ mol^{-1})	K136 (kJ mol^{-1})	R155 (kJ mol^{-1})
$\Delta\Delta G_{binding}$	−1.7	−5.1	−2.9
$\Delta\Delta G_{el,intra}$	2.2	3.0	1.4
$\Delta\Delta G_{el,sum}$	−2.5	−18.1	−2.9
$\Delta\Delta G_{solv}$	135.9	256.9	326

The change of the free energy of binding for the inhibitor Ac-DEDifEChaC-OH due to mutation of R109, K136, and R155, $\Delta\Delta G_{binding}$, was next calculated from the K_i values, experimentally determined on the mutant enzymes and shown in Figure 7. Table 5 summarizes the results. The attractive electrostatic interactions between the P1 carboxylate and the three basic amino acids are significantly smaller than the loss in solvation energy due to desolvation of these residues upon complex formation. In the complex R155 is almost completely buried by the P2 and P4 residues, which causes the unfavorable change in solvation energy. If only the intra- and intermolecular charge−charge interactions are considered, K136 makes the largest contribution to the interaction energy. The change in the intramolecular charge−charge interactions is unfavorable for the complex due to the change in the protonation state of H57 upon inhibitor binding and the resulting unfavorable interaction between the basic amino acids.

DISCUSSION

In the present work, we show that electrostatic interactions are dominant driving forces of substrate and inhibitor recognition by the NS3 protease. This conclusion is based on the following experimental results: (i) The NS3 protease shows a strikingly asymmetric surface charge distribution with a clustering of positively charged residues in the P5/P6 binding region and around the active site. These residues are highly conserved in all HCV isolates. Similarly, negatively charged residues are conserved around the P6 position of all NS3 substrates. (ii) K_m values of peptide substrates or K_i values of inhibitors increase with increasing NaCl concentration. These values depend on the presence of acidic residues in the P5/P6 region (and in the P1 region in the case of product inhibitors), and they are affected by mutagenesis of positively charged residues in the enzyme. (iii) Mutagenesis of positively charged residues in the enzyme or neutralization of negatively charged residues in the substrate peptide results in a decreased NaCl dependence of K_m values.

There are several examples of enzymes that predominantly utilize electrostatic interactions in the process of specific substrate recognition (*37*). In the case of acetylcholinesterase (*46*−*48*) or Cu,Zn superoxide dismutase (*49*−*51*), the catalytic groups are located at the bottom of a cleft into which substrate molecules are electrostatically attracted. These clefts generate dielectric discontinuities that magnify the local electrostatic potentials and lead to active site focusing effects (*52*). This mechanism is clearly not operative in the case of the NS3 protease that is characterized by a very flat substrate binding site. Binding pockets contribute to the specificity of a molecular recognition event by selecting ligands according to (among other features) shape complementarity. In the virtual absence of well-defined binding pockets in the NS3 protease, specificity appears to be conferred to the binding event through selection of ligands with electrostatic complementarity to the substrate binding site of the enzyme. This situation is unusual for proteases but not unique. In fact, electrostatically driven enzyme substrate complex formation was described for the aspartic protease pepsin (*53*, *54*). Among serine proteases, the situation found in NS3 is reminiscent of the thrombin exosites (*55*, *56*). This similarity is further underlined by the fact that both the NS3 protease and the thrombin exosite II display high affinities for the charged polysaccharide heparin.

In some proteins, the long-range character of electrostatic interactions is used to enhance the diffusion-limited association process of charged ligands (*46*−*52*). In such cases, the collision frequency of substrates with the complementary charged active site is increased with respect to the rest of the protein surface. Using a fluorescently labeled inhibitor, we obtained evidence for the occurrence of such an electrostatic precollision guidance as an important contribution to enzyme−ligand complex formation. The experimental data pointing to this mechanism are as follows: (i) The magnitude of the second-order association rate constant with the wild-type enzyme (1.5×10^8 M^{-1} s^{-1}) is close to the theoretical diffusion limit for molecules of this size. (ii) Increase of NaCl concentration or mutagenesis of crucial, charged residues in the enzyme decreases overall affinities by affecting association rate constants.

Analyzing our panel of point mutants, we found that most mutations had relatively weak effects. We identified K136 as the most important charged amino acid involved in the stabilization of the bound P1 α carboxylate, whereas K165, especially in concommittance with the R161S mutation, turned out to be important in the interaction with the P6 acid. Both residues are highly solvent exposed and have high thermal factors in the X-ray crystal structure, pointing to a considerable degree of conformational mobility. For individual residues to engage in ion pair interactions with oppositely charged substrate or inhibitor residues, they have to be both desolvated and "frozen" in a given conformation. Both processes are energetically unfavorable and indeed incomplete Coulombic compensation of desolvation or entropic effects explains why in some cases electrostatic interactions may actually oppose binding (*37*). In line with these considerations, calculations of the electrostatic interaction energies performed for the protease with a bound substrate or inhibitor showed that the charge−charge interactions between the oppositely charged amino acids of the protein and the ligand are more than compensated by a loss

of solvation energy. Both entropic and desolvation costs can be minimized if clusters of amino acids contribute to the generation of a diffuse, local electrostatic potential thereby avoiding the formation of individual ion pair interactions. This is in line with the observed, relatively weak effect of the single mutations and the incremental effects of double mutants. We think that formation of an only partially desolvated encounter complex accounts for the fact that electrostatics enhance association while disfavoring a precise anchoring of charged ligands. Still, substrate cleavage requires the correct positioning of the P1 amide, which would be difficult to achieve in a complex where the interaction is loose and not well-defined. We speculate that the lipophilic parts of the substrate, such as the P1 Cys close to the active site, form tighter interactions with the enzyme whereas the charged residues remain partially solvated. This is in agreement with the nature of the P1 specificity pocket, which is the only lipophilic site in the ligand binding region with a pocket-like appearance. We would like to emphasize the potential importance of this effect for inhibitor design. The structure−activity relationship of inhibitors with a high, electrostatically driven association rate can be analyzed by pre-steady-state kinetic measurements. The properties of these enzyme−inhibitor complexes may differ substantially from the structure activity relationship of inhibitors that do not exploit an electrostatic recognition mechanism. The latter may, in principle, have the same affinity but for completely different reasons. The affinity of uncharged ligands would not be dominated by the association rate but rather by the kinetic stability of the enzyme−inhibitor complex. In this case, pre-steady-state kinetic data are required to establish whether structure activity data can be transferred from one series to another and to evaluate the relevance of structural information.

In addition to influencing enzyme−ligand complex formation, charged residues in the vicinity of the active site and in particular K136 were shown to affect the k_{cat} value of the Pep5AB substrate. Surface charges were shown to influence the pK_a value of histidine residues in serine proteases (*57*, *58*), an effect that may influence k_{cat}. In addition, electrostatic interactions were also shown to directly contribute to the stabilization of catalytic transition states of serine proteases, an effect expected to become particularly important in enzymes with very asymmetric surface charge distributions (*59*). The transition state of the hydrolysis reaction involves the formation of a negatively charged, tetrahedral oxyanion intermediate that is stabilized by the active site oxyanion hole. The positive electrostatic potential arising from the vicinity of K136 may contribute to the stabilization of the negatively charged species during the transition state of the reaction and thus explains the influence of this residue on k_{cat}. The interaction energy between K136 and the transition-state oxyanion is partially compensated by a reduction of the pK_a of H57. Calculations considering different conformations of K136 suggest that the conformational flexibility of this amino acid is playing a role for catalysis. In support of the role of this residue in stabilizing charged transition states is also the dramatic effect of the K136M mutation on the inhibition of the NS3 protease by α-ketoacids (*60*). Ketoacids are mechanism-based inhibitors of serine proteases that are capable of transiently forming reversible covalent bonds with the active site serine (*61*, *62*). In the NS3 protease the stereochemistry of the nucleophilic attack by the active site serine differs from that observed with other serine proteases and is such that the oxyanion intermediate is formed outside the oxyanion hole (*39*). Stabilization of this unusual transition state presumably relies crucially on a local positive electrostatic potential and explains the large effects of mutations affecting this potential.

Extrapolation of the quantitative importance of electrostatic interactions during HCV polyprotein processing from the in vitro data presented in this work has to be done with some caution. In fact, we here report data on the interaction between a truncated domain and small peptides. In vivo, the relevant interactions occur between macromolecules bound to the membrane of the endoplasmic reticulum. Membrane association of both enzyme and substrates will influence diffusion phenomena, and the charged membrane surface is expected to affect the electrostatic potential of the substrate binding site of the NS3 protease. The effect of the membrane environment on the electrostatic properties of NS3 will have to be dissected using NS3/4A complexes (*63*, *64*) bound to membranes or phospholipid micelles.

REFERENCES

1. Kim, J. L., Morgenstern, K. A., Lin, C., Fox, T., Dwyer, M. D., Landro, J. A., Chambers, S. P., Markland, W., Lepre, C. A., O'Malley, E. T., Harbeson, S. L., Rice, C. M., Murcko, M. A., Caron, P. R., and Thomson, J. A. (1996) *Cell 87*, 343−355.
2. Love, R. A., Parge, H. E., Wickersham, J. A., Hostomsky, Z., Habuka, N., Moomaw. E. W., Adachi, T., and Hostomska, Z. (1996) *Cell 87*, 331−342.
3. Yan, Y., Li, Y., Munshi, S., Sardana, V., Cole, J., Sardana, M., Steinkühler, C., Tomei, L., De Francesco, R., Kuo, L., and Chen, Z. (1998) *Protein Sci. 7*, 837−847.
4. Yao, N., Hesson, T., Cable, M., Hong, Z., Kwong, A. D., Le, H. V., and Weber, P. C. (1997) *Nat. Struct. Biol. 4*, 463−467.
5. Kim, J. L., Morgenstern, K. A., Griffith, J. P., Dwyer, M., D., Thomson, J. A., Murcko, M. A., Lin, C., and Caron, P. R. (1998) *Structure 6*, 89−100.
6. Yao, N., Reichert, P., Taremi, S. S., Prosise, W., and Weber, P. C. (1999) *Structure 7*, 1353−1363.
7. Urbani, A., De Francesco, R., and Steinkühler, C. (1999) in *Proteases of Infectious Agents* (Dunn, B., Ed.) pp 61−91, Academic Press, San Diego.
8. Yao, N., and Weber, P. (1998) *Antiviral Ther. 3*, 93−97.
9. De Francesco, R., Pessi, A., and Steinkühler, C. (1999) *J. Viral Hepatitis 6*, 23−30.
10. Bartenschlager, R., Ahlborn-Laake, L., Mous, J., and Jacobsen, H. (1994) *J. Virol. 68*, 5045−5055.
11. Failla, C., Tomei, L., and De Francesco, R. (1994) *J. Virol. 68*, 3753−3760.
12. Lin, C., Thomson, J. A. and Rice, C. M. (1995) *J. Virol. 69*, 4373−4380.
13. Tanji, Y., Hijikata, M., Satoh, S., Kaneko, T. and Shimotohno, K. (1995) *J. Virol 69*, 1575−1580.
14. Steinkühler, C., Tomei, L. and De Francesco, R. (1996) *J. Biol. Chem. 271*, 6367−6373.
15. Shimizu, Y., Yamaji, K., Masuho, Y., Yokota, T., Inoue, H., Sudo, K., Satoh, S., and Shimotohno, K. (1996) *J. Virol. 70*, 127−132.
16. Steinkühler, C., Urbani, A., Tomei, L., Biasiol, G., Sardana, M., Bianchi, E., Pessi, A., and De Francesco, R. (1996) *J. Virol. 70*, 6694−6700.
17. Tomei, L., Failla, C., Vitale, R. L., Bianchi, E., and De Francesco, R. (1995) *J. Gen. Virol. 77*, 1065−1070.
18. Bianchi, E., Urbani, A., Biasiol, G., Brunetti, M., Pessi, A., De Francesco, R., and Steinkühler, C. (1997) *Biochemistry 36*, 7890−7897.

19. Urbani, A., Biasiol, G., Brunetti, M., Volpari, C., Di Marco, S., Sollazzo, M., Orrú, S., Dal Piaz, F., Casbarra, A., Pucci, P., Nardi, C., Gallinari, P., De Francesco, R., and Steinkühler, C. (1999) *Biochemistry 38*, 5206−5215.
20. Barbato, G., Cicero, D., Nardi, C., Steinkühler, C., Cortese, R., De Francesco, R., and Bazzo, R. (1999) *J. Mol. Biol. 289*, 371−384.
21. Steinkühler, C., Urbani, A., Tomei, L., Biasiol, G., Sardana, M., Bianchi, E., Pessi, A., and De Francesco, R. (1996) *J. Virol. 70*, 6694−6700.
22. Urbani, A., Bianchi, E., Narjes, F., Tramontano, A., De Francesco, R., Steinkühler, C. and Pessi, A. (1997) *J. Biol. Chem. 272*, 9204−9209.
23. Zhang, R., Durkin, J., Windsor, W. T., McNemar, C., Ramanathan, L., and Le, H. V. (1997) *J. Virol. 71*, 6208−6213.
24. Cicero, D., Barbato, G., Koch, U., Ingallinella, P., Bianchi, E., Nardi, C., Steinkühler, C., Cortese, R., Matassa, V., De Francesco, R., Pessi, A., and Bazzo, R. (1999) *J. Mol. Biol. 289*, 385−396.
25. La Plante, S. R., Cameron, D. R., Aubry, N., Lefebre, S., Kukolj, G., Maurice, R., Thibeault, D., Lamarre, D., and Llinas-Brunet, M. (1999). *J. Biol. Chem. 274*, 18618−18624.
26. Steinkühler, C., Biasiol, G., Brunetti, M., Urbani, A., Koch, U., Cortese, R., Pessi, A., and De Francesco, R. (1998) *Biochemistry 37*, 8899−8905.
27. Llinas-Brunet, M., Bailey, M., Fazal, G., Goulet, S., Halmos, T., Laplante, S., Maurice, R., Poirer, M., Poupart, M. A., Thibeault, D., Wernic, D., and Lamarre, D. (1998) *Bioorg. Med. Chem. Lett. 8*, 1713−1718.
28. Ingallinella, P., Altamura, S., Bianchi, E., Taliani, M., Ingenito, R., Cortese, R., De Francesco, R., Steinkühler, C., and Pessi, A. (1998) *Biochemistry 37*, 8906−8914.
29. De Francesco, R., Urbani, A., Nardi, M. C., Tomei, L., Steinkühler, C., and Tramontano, A. (1996) *Biochemistry 35*, 13282−13287.
30. Cerretani, M., Di Renzo, L., Serafini, S., Vitelli, A., Gennari, N., Bianchi, E., Pessi, A., Urbani, A., Colloca, S., De Francesco, R., Steinkühler, C., and Altamura, S. (1999) *Anal. Biochem. 266*, 192−197.
31. Fattori, D., Urbani, A., Brunetti, M., Ingenito, R., Pessi, A., Prendergast, K., Narjes, F., Matassa, V. G., De Francesco, R., and Steinkühler, C. (2000) *J. Biol. Chem. 275*, 15106−15113.
32. Hiromi, I. (1979) *Kinetics of Fast Enzyme Reactions*, pp 99−101, John Wiley & Sons, Inc.
33. Hallgren, T (1996). *J. Comput. Chem. 17*, 490−501.
34. Still, W. C., Tempcyk, A., Hawley, R. C. and Hendrickson, T. (1990) *J. Am. Chem. Soc. 112*, 6127−6129
35. Hallgren, T. A. (1996), *J. Comput. Chem. 17*, 520−552.
36. Honig, B., Sharp, K. A., and Yang, A.-S. (1993) *J. Phys. Chem. 97*, 1101−1110.
37. Honig B., and Nicholls A. (1995) *Science 268*, 1144−1149.
38. Sharp, K. A. (1998) *Proteins 33*, 39−48.
39. Barbato G., Cicero D. O., Cordier F., Narjes.F, Gerlach B., Sambucini S., Grzesiek S., Matassa V. G., De Francesco R., and Bazzo R. (2000) *EMBO J. 19*, 1195−206.
40. Di Marco S., Rizzi M., Volpari C., Walsh M., Narjes F., Colarusso S., De Francesco R., Matassa V. G., and Sollazzo M. (2000) *J. Biol. Chem. 275*, 7152−7157.
41. Hendsch, Z. S., and Tidor, B. (1994) *Protein Sci. 3*, 211−226.
42. Hendsch, Z. S., and Tidor, B. (1999) *Protein Sci. 8*, 1381−1392.
43. Cassidy, C. S., Ling, J., and Frey, P. (1997) *Biochemistry 36*, 4576−4584.
44. Sheinerman, F. B., Norel, R., and Honig, B. (2000) *Curr. Opin. Struct. Biol. 10*, 153−159.
45. Albeck, S., Unger, R., and Schreiber G. (2000) *J. Mol. Biol. 298*, 503−520.
46. Sussman, J., Harel, M., Frolow, F., Oefner, C., Goldman, A., Toker, L., and Silman, I. (1991) *Science 253*, 872−879.
47. Tan, R. C., Truong, T. N., McCammon, J. A., and Sussman, J. L. (1993) *Biochemistry 32*, 401−403.
48. Radic, Z., Kirchhoff, P. D., Quinn, D. M., McCammon, A., and Taylor, P. (1997) *J. Biol. Chem. 272*, 23265−23277.
49. Cudd, A., and Fridovich, I. (1982) *J. Biol. Chem. 257*, 11443−11447.
50. Getzhoff, E. D., Tainer, J. A., Weiner, P. K., Kollmann, P. A., Richardson, J. S., and Richardson, D. C. (1983) *Nature 306*, 287−290.
51. Desideri, A., Falconi, M., Polticelli, F., Bolognesi, M., Djinovic, K., and Rotilio, G. (1992) *J. Mol. Biol. 223*, 337−342.
52. Klapper, I., Hagstrom, R., Fine, R., Sharp, K., and Honig, B. (1986) *Proteins 1*, 47−59.
53. Pohl, J., and Dunn, B. (1988) *Biochemistry 27*, 4827−4834.
54. Kuzmic, P., Sun, C. Q., Zhao, Z. C., and Rich, D. (1991) *Tetrahedron 47*, 2519−2534.
55. Betz, A., Hofsteenge, J., and Stone, S. R. (1991) *Biochem. J. 275*, 801−803.
56. Sheehan, J. P., and Sadler, J. E. (1994) *Proc. Natl. Acad. Sci. U.S.A. 91*, 5518−5522.
57. Russell, A. J., and Fersht, A. (1987) *Nature 328*, 496−500.
58. DeSantis, G., and Jones, B. (1998) *J. Am. Chem. Soc. 120*, 8582−8586.
59. Jackson, S. E., and Fersht, A. R. (1993) *Biochemistry 32*, 13909−13916.
60. Narjes, F., Brunetti, M., Colarusso, S., Gerlach, B., Koch, U., Biasiol, G., Fattori, D., De Francesco, R., Matassa, V. G., and Steinkühler, C. (2000) *Biochemistry 39*, 1849−1861.
61. Walter, J., and Bode, W. (1983) *Hoppe-Seyler's Z. Physiol. Chem. 364*, 949−959.
62. Chen, Z., Li, Y., Mulichak, A. M., Lewis, S., and Shafer, J. A. (1995) *Arch. Biochem. Biophys. 322*, 198−203.
63. Sali, D. L., Ingram, R., Wendel, M., Gupta, D., McNemar, C., Tsarbopoulos, A., Chen, J. W., Hong, Z., Chase, R., Risano, C., Zhang, R., Yao, N., Kwong, A. D., Ramanathan, L., Le, H. V., and Weber, P. C. (1998) *Biochemistry 37*, 3392−3401.
64. Gallinari, P., Paolini, C., Brennan, D., Nardi, C., Steinkühler, C., and De Francesco, R. (1999) *Biochemistry 38*, 5620−5632.

BI002160T